In Vivo Assessment of Drug Efficacy against Mycobacterium abscessus Using the Embryonic Zebrafish Test System

Audrey Bernut, Vincent Le Moigne, Tiffany Lesne, Georges Lutfalla, Jean-Louis Herrmann, Laurent Kremer

In Vivo Assessment of Drug Efficacy against Mycobacterium abscessus Using the Embryonic Zebrafish Test System

Audrey Bernut, Vincent Le Moigne, Tiffany Lesne, Georges Lutfalla, Jean-Louis Herrmann and Laurent Kremer

Updated information and services can be found at:
http://aac.asm.org/content/58/7/4054

These include:

SUPPLEMENTAL MATERIAL	Supplemental material
REFERENCES	This article cites 43 articles, 17 of which can be accessed free at: http://aac.asm.org/content/58/7/4054#ref-list-1
CONTENT ALERTS	Receive: RSS Feeds, eTOCs, free email alerts (when new articles cite this article), more»

Information about commercial reprint orders: **http://journals.asm.org/site/misc/reprints.xhtml**
To subscribe to to another ASM Journal go to: **http://journals.asm.org/site/subscriptions/**

In Vivo Assessment of Drug Efficacy against *Mycobacterium abscessus* Using the Embryonic Zebrafish Test System

Audrey Bernut,[a] Vincent Le Moigne,[c] Tiffany Lesne,[a] Georges Lutfalla,[a] Jean-Louis Herrmann,[c] Laurent Kremer[a,b]

Laboratoire de Dynamique des Interactions Membranaires Normales et Pathologiques, CNRS UMR5235, Université Montpellier 2, Montpellier, France[a]; Inserm, DIMNP, Montpellier, France[b]; EA3647-EPIM, UFR des Sciences de La Santé, Université de Versailles St. Quentin, Montigny le Bretonneux, France[c]

Mycobacterium abscessus is responsible for a wide spectrum of clinical syndromes and is one of the most intrinsically drug-resistant mycobacterial species. Recent evaluation of the *in vivo* therapeutic efficacy of the few potentially active antibiotics against M. abscessus was essentially performed using immunocompromised mice. Herein, we assessed the feasibility and sensitivity of fluorescence imaging for monitoring the *in vivo* activity of drugs against acute M. abscessus infection using zebrafish embryos. A protocol was developed where clarithromycin and imipenem were directly added to water containing fluorescent M. abscessus-infected embryos in a 96-well plate format. The status of the infection with increasing drug concentrations was visualized on a spatiotemporal level. Drug efficacy was assessed quantitatively by measuring the index of protection, the bacterial burden (CFU), and the number of abscesses through fluorescence measurements. Both drugs were active in infected embryos and were capable of significantly increasing embryo survival in a dose-dependent manner. Protection from bacterial killing correlated with restricted mycobacterial growth in the drug-treated larvae and with reduced pathophysiological symptoms, such as the number of abscesses within the brain. In conclusion, we present here a new and efficient method for testing and compare the *in vivo* activity of two clinically relevant drugs based on a fluorescent reporter strain in zebrafish embryos. This approach could be used for rapid determination of the *in vivo* drug susceptibility profile of clinical isolates and to assess the preclinical efficacy of new compounds against M. abscessus.

The emerging pathogen *Mycobacterium abscessus* is the etiological agent of a wide spectrum of infections in humans, including severe chronic pulmonary and disseminated infections, mostly in immunosuppressed and cystic fibrosis (CF) patients (1), and cutaneous diseases, often posttraumatic and postsurgical. This neglected pathogen causes a higher fatality rate than other rapidly growing mycobacteria (RGM), and CF patient infections is becoming a major threat in most CF centers worldwide (2). *M. abscessus* infections occur in early childhood (3), are severe and sometimes fatal, especially following transplantation (4–6), and may lead to outbreaks of infection (6). It is also the main RGM responsible for nosocomial and iatrogenic infections in humans (postinjection abscesses, cardiac surgery, and plastic surgery) (7–9). It has been reported to cross the blood-brain barrier and cause important central nervous system (CNS) lesions. Although a rapid grower, *M. abscessus* possesses several important pathogenic traits, such as the ability to (i) persist silently for years and even decades in the human host (10) and to (ii) induce lung disease with caseous lesions and granuloma formation in the parenchyma (11, 12).

The major issue with *M. abscessus* relies on its intrinsic resistance to the most available antibiotics. The American Thoracic Society has recommended different groups of agents, namely, macrolides (clarithromycin), aminoglycosides (amikacin), cephamycins (cefoxitin), and carbapenems (imipenem), to treat *M. abscessus* infections (13). Patients with severe infections are generally treated with long courses of combinatorial antibiotic therapy, often backed by surgical resection. As antibiotic susceptibility testing is not fully standardized, the clinical response to drugs does not correlate well with *in vitro* susceptibility tests, and failure occurs frequently despite administration of two or three antibiotics for several months (14). This further emphasizes the need for suitable animal models (15, 16). In addition, different clinical isolates of this emerging pathogen are not uniformly susceptible to

currently used antibiotics (17). As a consequence, an optimal regimen to cure the *M. abscessus* infections has not been yet established.

Thanks to the recent availability of efficient genetic tools (18), *M. abscessus* has been proposed as an attractive experimental model to study nontuberculous mycobacterium-associated diseases. Our poor understanding of the pathogenesis of *M. abscessus*, essentially hampered by the restricted panel of cellular/animal models available, prompted us to develop the zebrafish (ZF) model of infection to evaluate *M. abscessus* infections (19). In particular, the *M. abscessus*/zebrafish model already provided important insights into *M. abscessus* pathogenesis, including the unexpected CNS tropism, a finding relevant in light of recent clinical studies reporting the presence of *M. abscessus* in the CNS of infected human patients (20, 21). Since infection foci/abscesses within the CNS, particularly the brain, appear very rapidly and are easily visualized, we reasoned that this alternative model could represent a valuable and cheap system to evaluate and compare the *in vitro* and *in vivo* activity of drugs against *M. abscessus*. Such a simple and innovative system would be particularly suited to screen active molecules and/or assess antibacterial activities for the discovery of the urgently needed drugs to fight *M. abscessus*.

Here, we report experimental conditions for spatiotemporal *in vivo* imaging of *M. abscessus* infections and their use to test the efficacy of drug treatments. This represents a unique biological model allowing noninvasive observations to evaluate, in real time, the efficacy of antibiotics in living infected vertebrates, a system that could be applied to high-throughput *in vivo* testing of drug efficacy against the most drug-resistant mycobacterial species.

MATERIALS AND METHODS

***M. abscessus* strains and growth conditions.** The rough variant of *M. abscessus sensu stricto* strain CIP104536[T] (ATCC 19977T) (R-*M. abscessus*) was grown at 30°C in Middlebrook 7H9 broth supplemented with 10% oleic acid-albumin-dextrose-catalase (OADC) enrichment and 0.05% Tween 80 (7H9[T]) or on Middlebrook 7H10 agar containing 10% OADC (7H10). Recombinant *M. abscessus* carrying pTEC27 (Addgene; plasmid 30182) that allows the expression of the tdTomato fluorescent protein under the control of a strong mycobacterial promoter was grown in the presence of 500 mg/liter hygromycin (19).

Mice experiments and CFU counting. BALB/c mice 6 to 8 weeks old were divided in groups of 5 to 7 mice and used for either intravenous (i.v.) or aerosol challenges. Inocula were prepared from rapidly thawed frozen aliquots, and bacterial clumps were eliminated by iterative passages through a 29.5-gauge insulin needle (Becton, Dickinson). Bacterial suspensions were then diluted in phosphate-buffered saline (PBS). For i.v. inoculations, 10^6 CFU (in 200 μl) was injected into the lateral tail/caudal vein, as previously described (22, 23). Pulmonary infections were achieved with aerosolized *M. abscessus* using an aerosol generator, equipped with a MicroMist small-volume nebulizer (Hudson RCI-Teleflex Medical) containing 6 ml of bacterial solution at 4×10^7 CFU/ml. Presleeping mice (isoflurane [Abbott]) were anesthetized with 200 μl of Hypnomidate (Etomidate [Janssen-Cilag]) and placed into an opened 50-ml syringe fixed on the top of a closed compartment containing the nebulizer. In this device, nebulization lasted for 15 min to vaporize the entire bacterial suspension. Lungs, livers, and spleens were collected in PBS and crushed, and 10-fold serial dilutions were plated on Middlebrook 7H11 plates for CFU counting, as previously described (22, 23). Plates were then incubated at 37°C for up to 7 days. The results were expressed as the mean $\log_{10}$ CFU per organ.

MICs. Antibiotic powders tested in drug susceptibility assays were pharmaceutical standards for imipenem-cilastatin (Mylan) or clarithromycin (Sigma-Aldrich). Stock solutions were dissolved in water (imipenem) or in dimethyl sulfoxide (DMSO) (clarithromycin). Drug susceptibility testing was also determined using the microdilution method, in cation-adjusted Mueller-Hinton broth, according to the Clinical and Laboratory Standards Institute (CLSI) guidelines (24). In addition, the susceptibility profile was also determined on LB agar supplemented with increasing concentrations of compounds. Serial 10-fold dilutions of each actively growing culture were plated and incubated at 37°C for 3 to 4 days, and the MIC was defined as the minimum concentration required to inhibit 99% of the growth.

Zebrafish care and ethic statements. All zebrafish experiments were done at the University Montpellier 2, according to European Union guidelines for handling of laboratory animals (http://ec.europa.eu/environment/chemicals/lab_animals/home_en.htm) and approved by the Direction Sanitaire et Vétérinaire de l'Hérault and Comité d'Ethique pour l'Expérimentation Animale de la Région Languedoc Roussillon (CEEA-LR) under the reference CEEA-LR-13007. Experiments were done using the golden ZF mutant (25), maintained as described earlier (19). Ages of embryos are expressed as hours postfertilization (hpf).

Microinjection of *M. abscessus* into embryos. Mid-log-phase cultures of *M. abscessus* expressing tdTomato were centrifuged, washed, and resuspended in PBS supplemented with 0.05% Tween 80 (PBS[T]). Bacterial suspensions were then homogenized through a 26-gauge needle and sonicated, and the remaining clumps were allowed to settle for 5 to 10 min, as previously described (19). Bacteria were concentrated to an opti-

cal density at 600 nm (OD$_{600}$) of 1 in PBS[T] and i.v. injected (≈2 nl containing 300 CFU) into the caudal vein in 30-hpf embryos previously dechorionated and anesthetized. To follow infection kinetics and embryo survival, infected larvae were transferred into 96-well plates (2 embryos/well) and incubated at 28.5°C. The inoculum size was checked by injection of 2 nl in sterile PBS[T] and plated on 7H10 supplemented with 500 mg/liter hygromycin.

Drug efficacy assessment in *M. abscessus*-infected ZF. Clarithromycin and imipenem-cilastatin were added at 1 day postinfection (dpi), directly into the water containing the embryos. Three doses were tested, corresponding to 1.7×, 17×, and 170× the MIC of clarithromycin and 0.5×, 5×, or 28× the MIC of imipenem, based on the values determined using the microdilution method (see Table S1 in the supplemental material). *In vivo* drug efficacy was determined for each concentration by following (i) bacterial burdens, (ii) kinetics of embryo survival, (iii) evolution of the infection foci/abscesses within the CNS, and (iv) effect on bacterial cord formation/reduction. Survival curves were determined by recording dead embryos (no heartbeat) every day for up to 13 days. Regarding the kinetic of mycobacterial loads, groups of three infected embryos were collected, lysed individually in 2% Triton X-100–PBS[T] with a 26-gauge needle, and resuspended in PBS[T]. Several 10-fold dilutions of homogenates were plated on 7H10 containing 500 mg/liter hygromycin and BBL MGIT PANTA (Becton, Dickinson), used as recommended by the supplier. CFU were enumerated after 4 days of incubation at 30°C. This procedure was repeated at 0, 3, and 5 dpi.

Microscopy. Wide-field, bright-field, and fluorescence live microscopy of infected embryos was performed using an Olympus MVX10 epifluorescence microscope equipped with an X-Cite120Q (Lumen Dynamics) 120-W mercury light source. Images were acquired with a digital color camera (Olympus XC50) and processed using CellSens software (Olympus). A tetramethyl rhodamine isocyanate (TRITC)-MVX10 fluorescence filter cube was used for detection of red light. For live imaging, anesthetized infected embryos were positioned in dishes and immobilized with 1% low-melting-point agarose solution covering the entire larvae, and then immobilized embryos were immersed with fish water containing tricaine for direct visualization.

Image processing and analysis. Final image analysis and visualization were performed using GIMP 2.6 freeware to merge fluorescent and differential inference contrast (DIC) images and to adjust levels and brightness and to remove out-of-focus background fluorescence.

Statistical analyses. Statistical analyses of comparisons between Kaplan-Meier survival curves were performed using the log-rank test with Prism 4.0 (GraphPad, Inc.). CFU counts and quantification experiments were analyzed using one-way analysis of variance (ANOVA) and Fisher's exact test, respectively. Statistical significance was assumed at P values of <0.05.

RESULTS

***M. abscessus* fails to establish a persistent infection in BALB/c mice.** Experiments were first aimed at determining the colonization rate of R-*M. abscessus* in a murine pulmonary infection model (Fig. 1A). Aerosol infections of BALB/c mice led to an initial and rapid increase of the bacterial burden from 1 to 3 days postinfection (dpi) in the lungs, followed by a phase of infection control leading to a reduction (starting after 3 dpi) and almost complete clearance of the bacilli at 27 dpi. Very few bacteria were detected within the spleen or the liver of infected mice. The colonization profile after i.v. challenge showed that bacilli were found primarily in the liver at 1 dpi and to a lesser extent in the spleen and lungs (Fig. 1B). All heavily infected organs rapidly underwent a progressive reduction in bacterial loads with a 3-$\log_{10}$ CFU decrease in the liver and lungs at 30 dpi, highlighting a transient colonization process. This indicates that immunocompetent mice steadily eradicate the pathogen and therefore that wild-type BALB/c mice
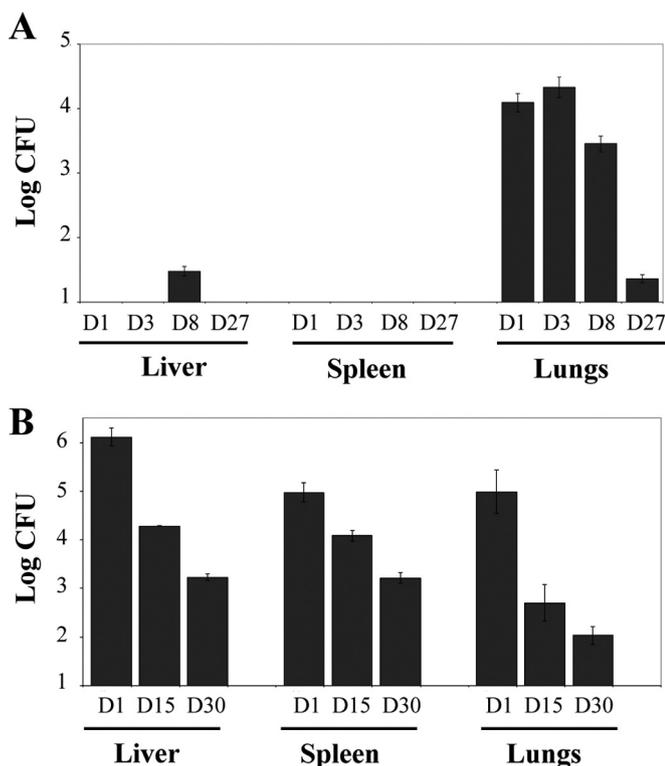
FIG 1 Kinetics of colonization of *M. abscessus* in aerosolized or intravenously infected BALB/c mice. (A) Mice were aerosolized by 4×10^7 CFU/ml of R-*M. abscessus*. Animals were then sacrificed at days 1, 3, 8, and 27 prior to CFU counting in the liver, spleen, and lungs. Results are expressed as the log units of CFU. (B) Mice were challenged i.v. with 10^6 CFU of R-*M. abscessus*. Animals were then sacrificed at days 1, 15, and 30 to determine the CFU counts in the different organs. Results are expressed as mean $\log_{10}$ CFU from 2 to 3 independent experiments ($n = 5$ to 7 mice for each time point). Error bars represent the standard errors of the means (SEM).

are not well adapted to investigate the *in vivo* efficacy of therapeutic treatments. This would require testing a very large number of animals to ensure that the observed CFU decrease results from an antibiotic regimen rather than from the natural course of infection. This highlights the need for an alternative animal model, susceptible to *M. abscessus* infection, permissive to bacterial replication, and leading to the development of infection foci/abscesses and death. Therefore, the ZF embryo model was chosen to test *in vivo* assessments of drugs against *M. abscessus*.

Zebrafish larvae for *in vivo* assessment of drug activity in *M. abscessus*. An experimental protocol was designed to assess *in vivo* antimycobacterial drug activity against *M. abscessus* in ZF larvae (Fig. 2). Red fluorescent tdTomato-expressing R-*M. abscessus* was injected in the caudal vein of embryos at 30 h postfertilization (hpf) and transferred into 96-well plates. Antibiotics were directly added at 1 dpi to the water containing the infected embryos, and the drug-supplemented water was then changed on a daily basis for 5 days. Thanks to the optical transparency of the embryos, daily microscopic recording of mortality (transmission) and bacterial burden (fluorescence) were used as phenotypic readouts. We have previously shown that the rough *M. abscessus* exhibits a marked neurotropism with massive abscesses within the CNS (19), thus prompting us to assess the chemotherapeutic activity of drugs in *M. abscessus*-infected embryos with a special emphasis on
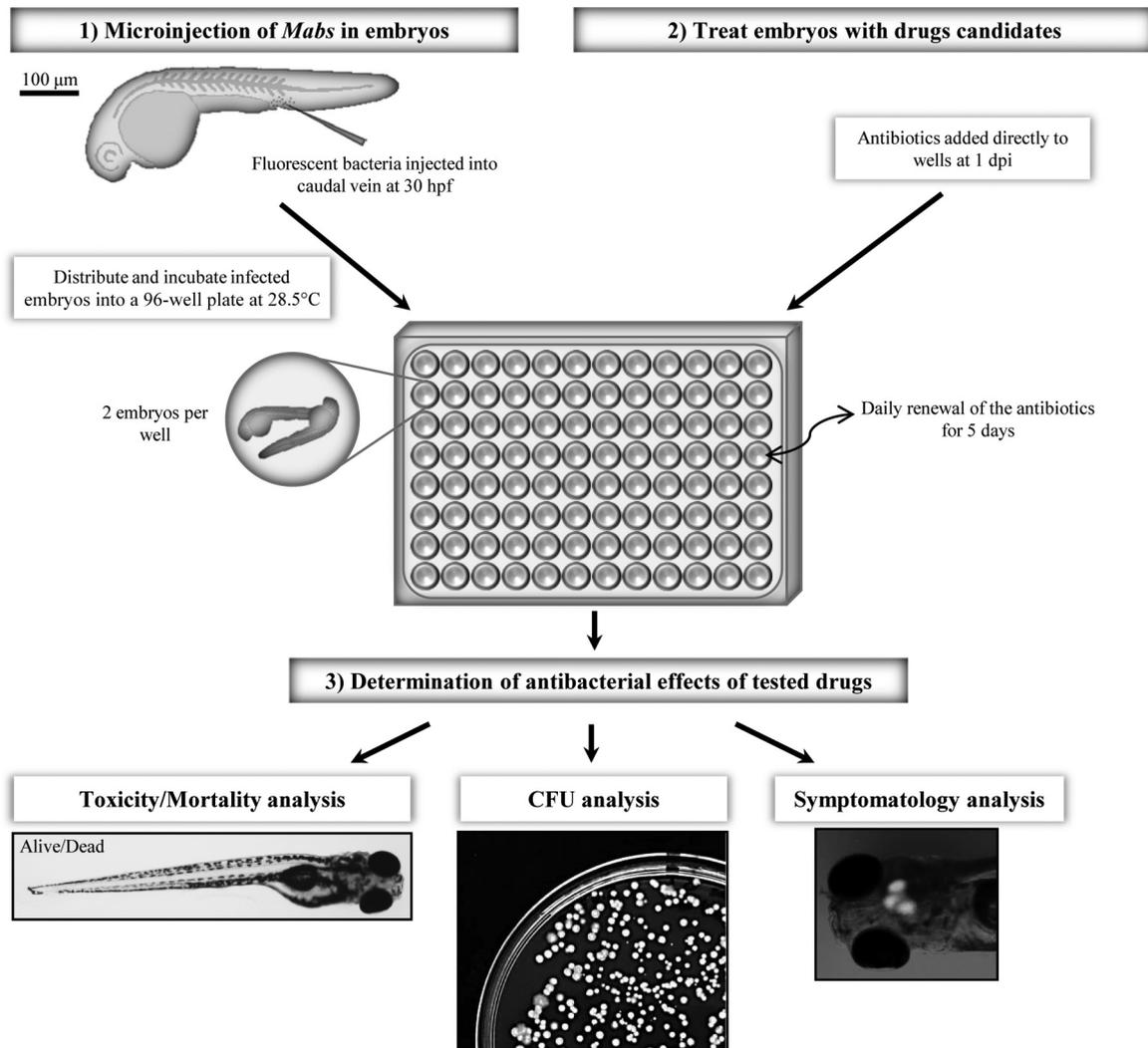
infection within the CNS (Fig. 2). Drug-mediated toxicity was investigated by checking survival curves of noninfected embryos treated with increasing drug doses.

MICs of antimycobacterial drugs against *M. abscessus*. We first determined the *in vitro* activity of various drugs, including antitubercular agents, against *M. abscessus* using microdilution in cation-adjusted Mueller-Hinton broth, according to the Clinical and Laboratory Standards Institute guidelines (24). Table S1 in the supplemental material shows that the activity varies considerably, in agreement with other studies (17). The first-line antitubercular drug isoniazid and second-line drug thioacetazone appeared inactive against *M. abscessus*. Among the few clinically used drugs for the treatment of *M. abscessus* infection, cefoxitin, amikacin, imipenem, and erythromycin exhibit moderate activity *in vitro* on agar plates, with MICs ranging from 60 to 125 μM, whereas clarithromycin demonstrated the highest activity with an MIC value of 4 μM. Because clarithromycin and imipenem exhibit different physicochemical properties (high molecular weight and hydrophobicity for clarithromycin versus low molecular weight and hydrophilicity for imipenem), they were further investigated for their *in vivo* therapeutic efficacy in *M. abscessus*-infected ZF.

***In vivo* susceptibility of *M. abscessus* to clarithromycin.** Due to poor information concerning the mechanisms of drug uptake by ZF embryos/larvae, we tested a wide range of clarithromycin concentrations: 6.6 μM to 668 μM ($1.7\times$ to $170\times$ the *in vitro* MIC value from the microdilution method). Supplementing the embryo-containing water with low or intermediate doses ($1.7\times$ and $17\times$ the MIC, respectively) led to no toxicity, as measured by larval survival, while the highest tested dose ($170\times$ MIC) led to a 10% reduction in larval survival at 9 dpi, with respect to that of the control group (water with 1% DMSO; Fig. 3A) (26). In the presence of high doses of clarithromycin, embryos had a curved body trunk with uninflated swim bladders (Fig. 3A, inset). These phenotypic alterations were hardly observed when exposed to intermediate or low doses of clarithromycin (not shown).

No significant increased survival was found when infected embryos were exposed to low and intermediate drug concentrations (Fig. 3B). In contrast, high doses extended the lifespan of infected embryos and fully protected the infected embryos up to 9 dpi, when the first embryo started to die, which coincidently corresponded to the toxicity-induced killing effect (Fig. 3A). This shows that clarithromycin, using the highest regimen, is efficient in the ZF test system.

Effects of clarithromycin on ZF survival, bacterial burden, and abscesses. Increased survival was associated with lower bacterial burdens after 3 dpi in the presence of the highest dose ($170\times$ MIC), as determined quantitatively by CFU plating (Fig. 3C), whereas treatment with the low or intermediate doses failed to restrict mycobacterial growth. *In vivo* drug efficacy was next monitored by time-lapse fluorescence microscopy (Fig. 3D) of the rapidly growing infection foci and abscesses in the larval brain (19). Imaging the same infected embryos at 3 and 5 dpi revealed that abscesses within the brain were already reduced at 3 dpi when treated with high drug concentrations, and this reduction of the clinical signs of infection was even more accentuated at 5 dpi. Consistent with the survival curves and kinetic of bacterial growth, there was no visible reduction of the infection at 5 dpi in ZF treated with low or intermediate drug concentrations. Quantitative analysis reveals that high doses of clarithromycin reduced

1) Microinjection of *Mabs* in embryos

100 μm

Fluorescent bacteria injected into caudal vein at 30 hpf

Distribute and incubate infected embryos into a 96-well plate at 28.5°C

2 embryos per well

2) Treat embryos with drugs candidates

Antibiotics added directly to wells at 1 dpi

Daily renewal of the antibiotics for 5 days

3) Determination of antibacterial effects of tested drugs

Toxicity/Mortality analysis

Alive/Dead

CFU analysis

Symptomatology analysis

FIG 2 Experimental protocol to assess the *in vivo* drug activity on *M. abscessus* infection. (1) ZF embryos were i.v. infected with ≈300 CFU of R-*M. abscessus* expressing tdTomato and distributed and incubated into 96-well plates. From 1 dpi, embryos were exposed to the drugs of interest, which were directly added to the wells. (2) Drugs were then removed and renewed daily for 5 days. (3) To determinate the *in vivo* antibacterial effects of the drugs, the embryo survival, the bacterial loads, and the evolution of the infection process were monitored at a spatiotemporal level by videomicroscopy.

by 50% the number of embryos with abscesses (Fig. 3E) both in the brain and the spinal cord (Fig. 3F). This indicates that clarithromycin exerts a therapeutic effect by inhibiting mycobacterial growth, preventing the development of abscesses within the CNS, and protecting the embryos from bacterial killing.

Effects of imipenem on ZF survival and reduction of the pathological signs. Imipenem is a clinically relevant drug against *M. abscessus* known to act on L,D-transpeptidases (17, 27). Concentrations from 0.5× to 28× MIC of imipenem were tested, which all failed to display signs of toxicity-induced killing or developmental abnormalities (data not shown). When assessing the effect of imipenem on infected ZF, no increased survival was found with low drug concentrations. However, treatment with intermediate doses led to a significant increase in survival, and 100% of protection was observed in the presence of the highest drug concentration (Fig. 4A). These survival rates correlated with CFU loads as intermediate and high doses of imipenem started to restrict bacterial growth at 3 dpi (after 2 days of drug treatment)

(Fig. 4B). With the highest dose, there was a 3-$\log_{10}$ decrease in CFU at 5 dpi (4 days of treatment) compared with that of the untreated control group. Time-lapse fluorescence microscopy further confirmed the *in vivo* efficacy of imipenem at intermediate and high doses, illustrating the inhibition of bacterial growth and disappearance of abscesses in the larval brain at 3 and 5 dpi, respectively (Fig. 4C). High doses significantly reduced the proportion of embryos with abscesses (Fig. 4D), a phenotypic effect that was particularly apparent in the brain on infected embryos (Fig. 4E), indicating that imipenem reduces the pathology signs of the infection.

These results prompted us to check whether imipenem can counteract/alter the progression of an already established infection, if given at 3 dpi when brain abscesses are already apparent (see Fig. S1A in the supplemental material). Death curves indicate that treatment with high doses of imipenem efficiently extended the lifespan of embryos with preexisting abscesses (see Fig. S1B). A large proportion (more than 60%) of the treated embryos sur-
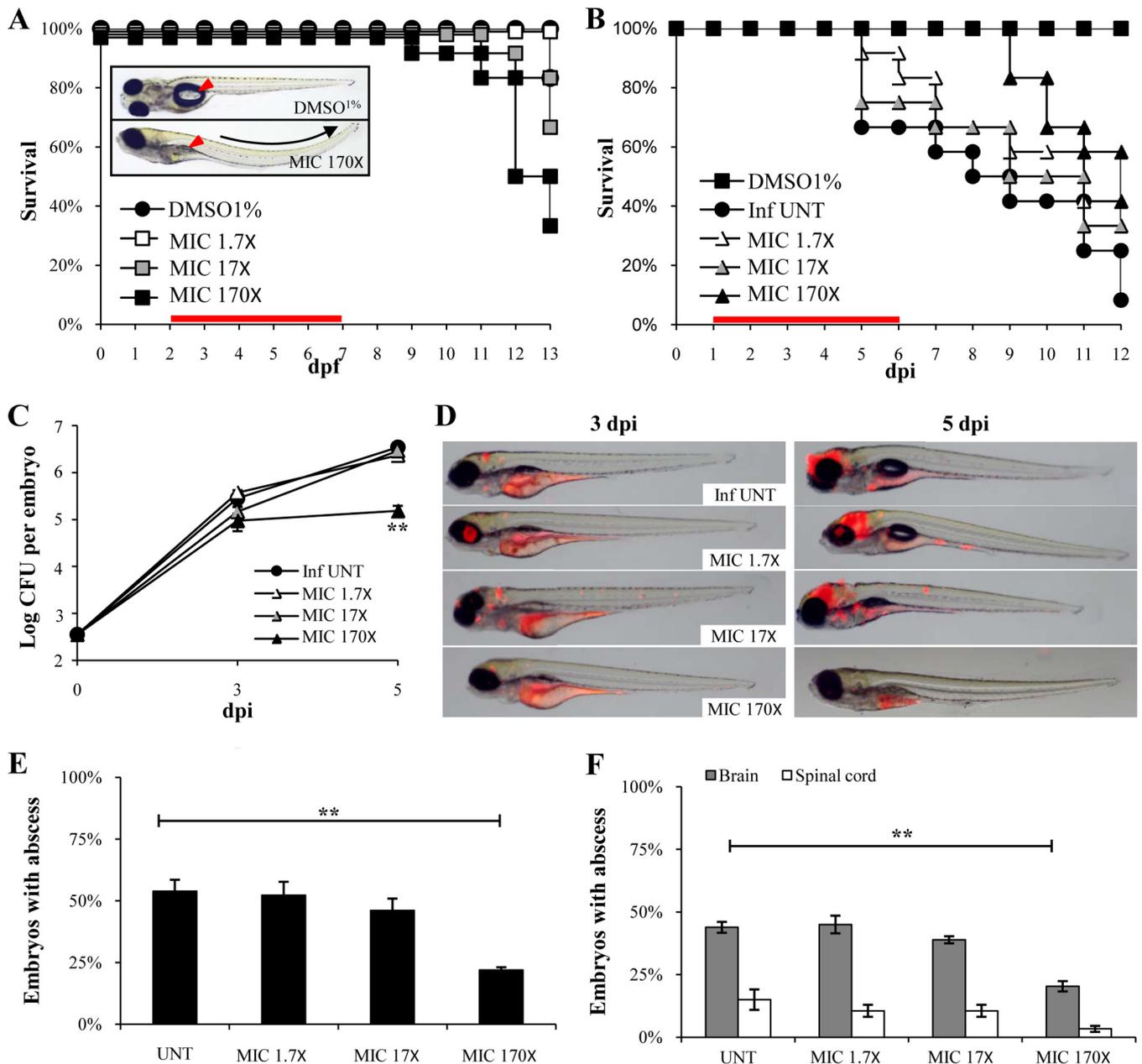
FIG 3 *In vivo* characterization of clarithromycin activity on *M. abscessus* infection. (A to F) Embryos were soaked in clarithromycin at 1.7×, 17×, or 170× the MIC for 5 days. The red bar indicates the start and duration of treatment. (A) Survival of uninfected embryos treated with various doses of clarithromycin and compared to mock controls (DMSO 1%) ($n = 20$ for each, representative of three independent experiments). Representative microscopy image of an untreated (inset, top) or drug-treated embryo (inset, bottom) at 8 dpf. Clarithromycin appears toxic at the highest concentration, as evidenced by the development of abnormalities and the increased mortality rate in the drug-exposed embryos compared to that of the mock control ($P = 0.028$, log-rank test). (B) Survival of *M. abscessus*-infected embryos treated at various doses of clarithromycin and compared to untreated infected embryos ($\approx$300 CFU, $n = 20$, representative of three independent experiments). A significant increased survival was observed in the infected embryos exposed to the highest drug concentration ($P = 0.029$, log-rank test). (C) Bacterial loads of untreated or treated embryos ($\approx$400 CFU). Results are expressed as mean $\log_{10}$ CFU per embryo from three independent experiments. A significant reduction in bacterial burdens with 170× the MIC in drug treated-embryos is observed at 5 dpi. (D) Spatiotemporal visualization of the infection by *M. abscessus* expressing dtTomato ($\approx$300 CFU) in untreated or drug-treated embryos. The representative fluorescence and transmission overlays of whole embryos are shown. The yolk is autofluorescent. (E) Frequency of abscesses in whole untreated or drug-treated embryos over 13 dpi ($\approx$300 CFU; average of three independent experiments). Infected embryos developed significantly fewer abscesses in the presence of clarithromycin at 170× the MIC than untreated infected embryos. (F) Average localization of abscesses of the infected embryos in panel E. *M. abscessus*-infected ZF developed significantly fewer abscesses than untreated infected ZF within the brain and the spinal cord when exposed to the highest clarithromycin dose. For panel C, statistics were calculated using one-way ANOVA; for panels E and F, Fisher's exact test was used, comparing each category of drug-treated embryos to untreated controls. Error bars represent the SEM. **, $P < 0.01$.
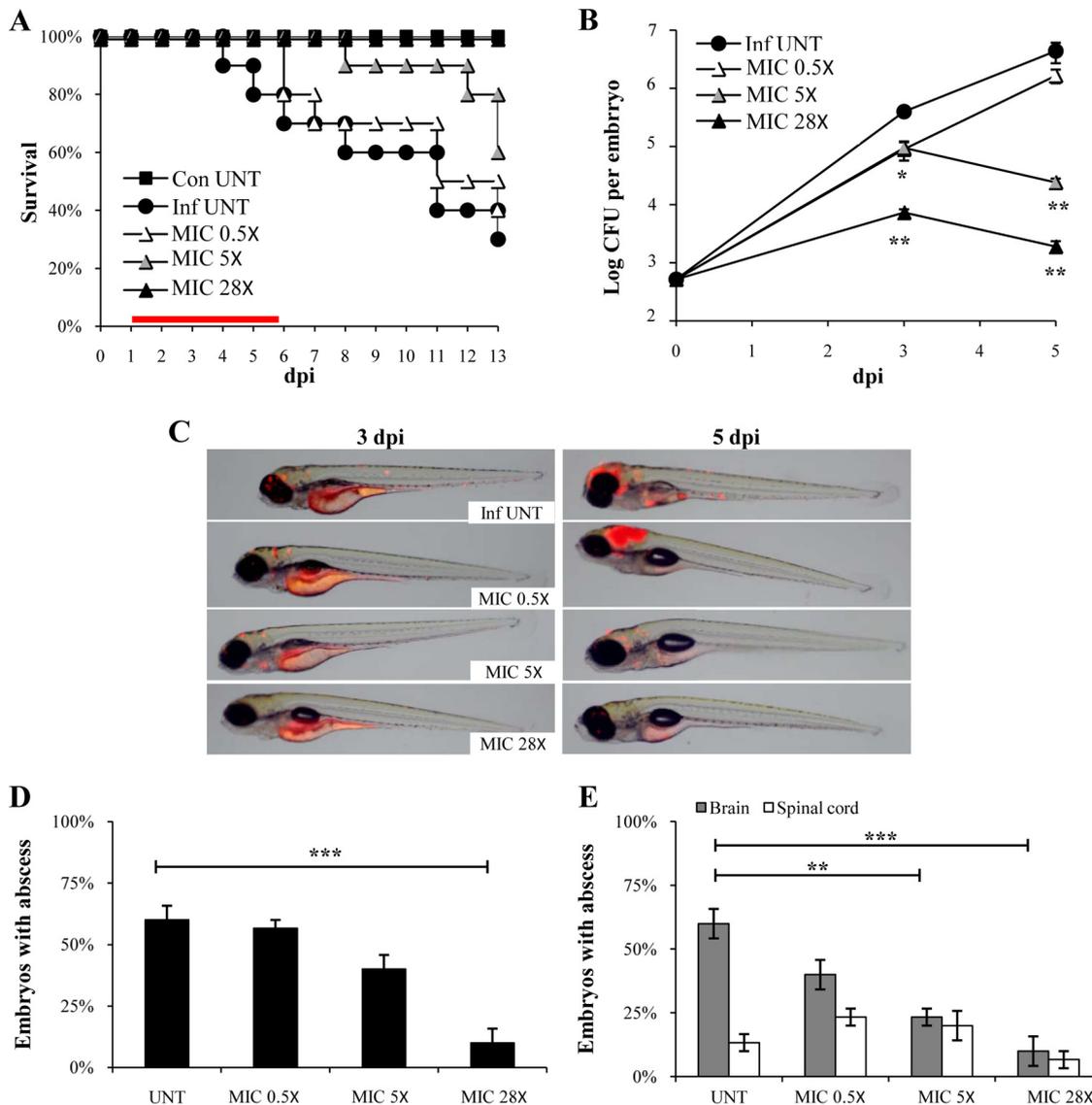
FIG 4 Imipenem treatment cures *M. abscessus*-infected embryos. (A to E) From 1 dpi, embryos were exposed for 5 days to imipenem concentrations corresponding to 0.5×, 5×, or 28× the MIC. (A) Survival of R-*M. abscessus*-infected embryos treated at various doses of imipenem and compared to untreated infected embryos (≈300 CFU, n = 20, representative of three independent experiments). Survival of treated R-*M. abscessus*-infected embryos is dose dependent. Significant increased survival was observed in infected embryos exposed to 5× and 28× MIC of imipenem. The red bar indicates the start and duration of treatment. (B) Bacterial loads of untreated or imipenem-treated embryos (≈400 CFU). Results are expressed as mean $\log_{10}$ CFU per embryo from three independent experiments. A significant decrease of bacterial load was observed after 3 dpi in the 28× MIC imipenem-treated embryos. (C) Spatiotemporal visualization of the infection by R-*M. abscessus* expressing tdTomato (≈300 CFU) in untreated or imipenem-treated embryos. The representative fluorescence and transmission overlays of whole embryos are shown. (D) Frequency of abscesses in whole untreated or imipenem-treated embryos over 13 dpi (≈300 CFU, average of three independent experiments). Only the 28× MIC imipenem-treated embryos developed significantly fewer abscesses than untreated-infected embryos. (E) Average localization of abscesses of the infected embryos in panel D. Five times and 28× MIC of imipenem-treated embryos infected by *M. abscessus* developed fewer abscesses within the brain than untreated infected embryos. For panel B, statistics were calculated using one-way ANOVA; for panels D and E, Fisher's exact test was used, comparing each category of imipenem-treated embryos to untreated controls. Error bars represent the SEM. *, $P = 0.02$; **, $P < 0.01$; ***, $P < 0.001$.

vived the infection compared to 10% for the nontreated individuals ($P = 0.008$). The 40% of embryos that died despite treatment showed increased bacterial loads in the CNS (data not shown). The increased index of protection rate was associated with a significant decrease in the number of embryos with abscesses (see Fig. S1C), particularly within the brain (see Fig. S1D). This "curative" protocol shows that imipenem was able to cure embryos with preexisting abscesses and protect severely infected ZF.

In vivo inhibition activity of imipenem on mycobacterial cording. Rough *M. abscessus* displays a dry texture with organized serpentine cords on agar plates (19, 28, 29) and large bacterial clumps consisting mainly of cords in liquid cultures (19). Our recent studies also unraveled the presence of serpentine cords within the brain or spinal cord of embryos infected with the rough morphotype and emphasized the role of cording in immune evasion by preventing phagocytosis of *M. abscessus* by macrophages
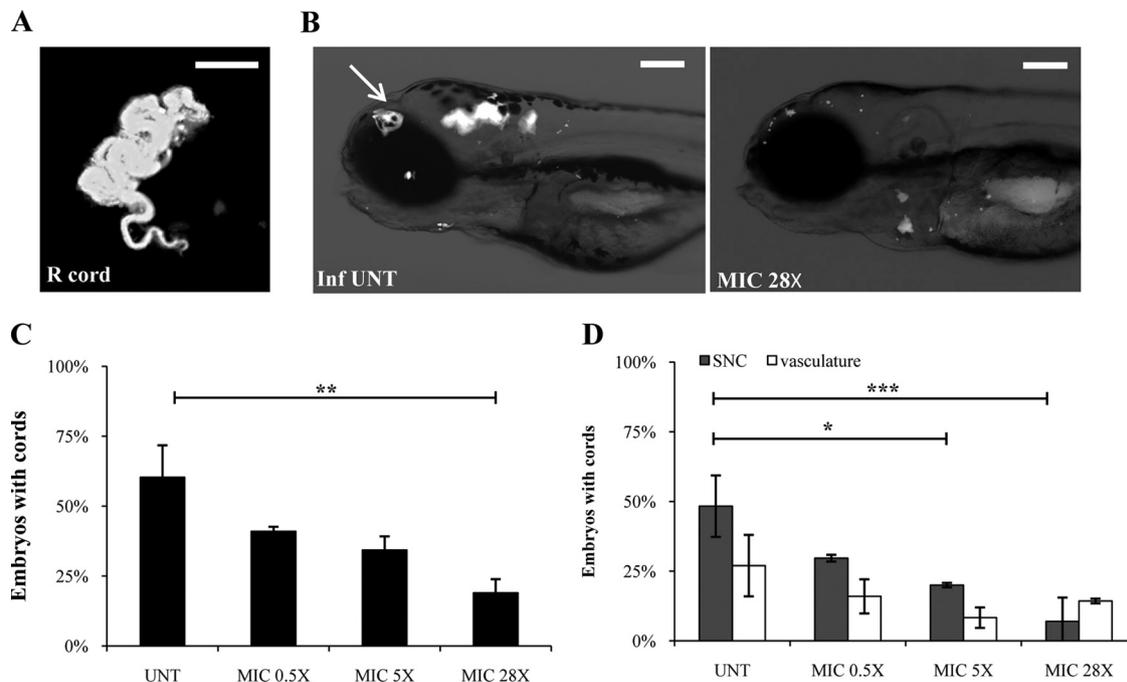
FIG 5 Imipenem treatment decreases the early pathophysiological signs within the CNS. (A to D) tdTomato-expressing R-*M. abscessus* (≈300 CFU) was injected in 30-hpf embryos (*n* = 15, average of three independent experiments). From 1 dpi, embryos were exposed to imipenem at 0.5×, 5×, or 28× MIC for 5 days. (A) Fluorescence microscopy of a typical R serpentine cord. Scale bar, 100 μm. (B) Fluorescence and DIC overlay of whole heads of 28× MIC imipenem-treated and untreated infected embryos with fluorescent R-*M. abscessus* showing serpentine cord (white arrow). Scale bars, 100 μm. (C) Percentage of embryos with cords in whole untreated and imipenem-treated embryos at 4 dpi. A significant reduction in the proportion of embryos with cords was observed when embryos were treated with the highest (28× MIC) imipenem concentration. (D) Average localization of cord within the infected embryos in panel C. Infected embryos treated with the intermediate (5× MIC) and high (28× MIC) imipenem doses developed significantly fewer serpentine cords within the CNS than untreated infected embryos. For panels C and D, statistics were calculated using Fisher's exact test comparing each category of imipenem-treated embryos to untreated control. All results are expressed as the averages from three independent experiments, and error bars represent the SEM.

and neutrophils (19). Cords are easily visualized and counted by fluorescence microscopy (Fig. 5A), and they promote extracellular replication, abscess formation, and tissue damage (19). We checked whether exposure of infected embryos to imipenem may affect the development of mycobacterial cords. Figure 5B shows the impact of imipenem treatment on the number of cords; quantitative analysis is shown in Fig. 5C. The presence of low doses of imipenem has little impact on mycobacterial cords, although a reduction of the number of embryos with cords was detected at 4 dpi. However, this effect was more pronounced with higher drug concentrations, with only 20% of cord-laden embryos at 4 dpi (compared to 60% for untreated embryos at 4 dpi). This dose-dependent effect occurred essentially within the CNS, while reduction of cord formation within the vasculature was not significant (Fig. 5D).

DISCUSSION

At a basic research level, the appropriate use of animal models can help to improve our understanding of host-pathogen interactions. At a more applied level, preclinical evaluation of new drugs requires *in vivo* testing prior to progressing along the development pipeline. However, *in vivo* animal studies, when possible, are usually costly and time-consuming and present a major bottleneck in drug developments. Implementation of novel approaches, expected to accelerate the *in vivo* assessment of drugs, is particularly justified in two cases. First, such systems are useful for bacterial infections requiring extended periods of drug treatment, such as

mice infected with *M. tuberculosis*, for which rapid *in vivo* assessment of drug efficacy directly in infected mice using fluorescence imaging (30) or using improved firefly luciferase (31) was elegantly demonstrated. We similarly show in this study how the use of fluorescence imaging can be useful in evaluating antimicrobial activity against *M. abscessus*. Second, alternative biological systems are particularly relevant for infections lacking a permissive animal model. In this context, we recently demonstrated the high susceptibility of ZF embryos to *M. abscessus* (19) and how the number of CNS abscesses may represent a marker for establishing *in vivo* antibiotic activity against *M. abscessus*.

One of the key steps of the drug discovery process is to identify and evaluate the *in vitro* and *in vivo* potential of new hits against *M. abscessus* using adapted animal models. The murine model in immunocompetent BALB/c mice (i.v. or aerosol infections) led only to transient colonization, impeding its use as a valuable animal model for drug testing. Comparatively, the SCID mouse model has been shown to produce a chronic infection of *M. abscessus*, but this model has not been used for drug testing (29, 32). Granulocyte-macrophage colony-stimulating (GM-CSF) knockout (KO) mice have recently been used to develop a new animal model of persistent pulmonary *M. abscessus* infection that can be used for preclinical efficacy testing of antimicrobial drugs (15). Azithromycin treatment of *M. abscessus*-infected GM-CSF KO mice resulted in a lower bacterial burden in the lungs and spleen, weight gain, and significant improvement in lung pathology (15). Another report proposed nude mice as an adequate model for *in*

vivo chemotherapy studies (16). However, both models raised the question of the adaptive response in addition to the antibiotic activity in eradicating the bacilli. It was previously shown that, albeit being a rapid-growing mycobacterium, *M. abscessus* infection was controlled only in mice with a functional adaptive immune response (22), compared to *Mycobacterium chelonae*, which was cleared even in T cell-deficient mice. Despite the fact that immunocompromised mice present a significant advance compared to wild-type mice in preclinical assessments, they remain costly, time-consuming, and, most likely, not suitable for general use in drug screening strategies.

New nonmammalian models of infection have been developed, including for *Drosophila melanogaster* (33, 34), *Caenorhabditis elegans* (35), or *Danio rerio* (36, 37), offering advantages in terms of speed, cost, technical convenience, and ethical acceptability over the mouse model. Except for the recent *Drosophila* model (34), these models have not been reported for antibiotic assessments against *M. abscessus*. We propose here the ZF model to visualize, by noninvasive imaging, the progressive infection of *M. abscessus* in live animals and to quantify the effect of drug treatment. We successfully investigated the suitability and sensitivity of two clinically relevant drugs, clarithromycin and imipenem, to visualize in dose- and time-dependent manners the dynamics of cord and abscess formation/resorption. One major advantage of this model, compared to mice, is the ease and rapidity of experimentation within a restricted time scale and low cost. That both drugs had a positive impact in terms of embryo survival was correlated to a significant reduction in the number of CFU and abscesses, demonstrating a proof of concept that ZF embryos are suitable for drug efficacy testing. Since *in vitro* studies demonstrated decreased MICs in the presence of imipenem, for clarithromycin, minocycline, levofloxacin, and moxifloxacin (38), future work should also address the *in vivo* efficacy of these drug combinations using the *M. abscessus*/ZF couple.

It is, however, noteworthy that despite their unique features for *in vivo* drug testing, ZF embryos also present several disadvantages over mammalian models. In particular, there are some important anatomical differences between ZF embryos and mammals, such as gills instead of lungs, hematopoiesis occurring in the anterior kidney instead of the bone marrow, lack of discernible lymph nodes, as well as a very different reproductive system. The natural lack of adaptive immunity early in the development is very likely to affect the outcome of the infection, thus making it difficult to directly correlate data obtained in ZF and in humans. In addition, as shown in this study, embryos are adapted to testing antibiotics during acute R-*M. abscessus* infections but not during the chronic stages of the disease, which can be better modeled, for instance, using immunocompromised mice (15). Since pharmacokinetics are not known in ZF, it remains difficult at this stage to directly transpose the MIC data obtained in ZF to humans. As a consequence, this biological system should essentially be regarded as an early model for preclinical drug testing and/or to select new active compounds, which should then be evaluated in other models before clinical trials.

The perspectives of application of the present findings are multiple. First, this method could be implemented to address the *in vivo* drug susceptibility profiles of clinical isolates, including strains from CF and non-CF patients, as *M. abscessus* clinical strains are not uniformly susceptible to currently used antibiotics. Due to these strain-to-strain variations (17, 39), no optimal regimen has been established to cure *M. abscessus* infections, and determining the susceptibility/resistance profile of clinical strains may greatly help the clinician to select optimal drug treatments. It is worth mentioning that for this particular application, no absolute requirement for the tested strains to carry pTEC27 is needed, as visualization of fluorescent bacteria is not necessary if only assessing ZF survival. Second, since the ZF is particularly amenable to mimic a CF-like microenvironment, by silencing the *cftr* expression level (40), this system could be used to compare the therapeutic efficacy of clarithromycin and imipenem (and perhaps other antibiotics) in a *cftr*-deficient environment, as it remains to be established whether a defect in CFTR affects susceptibility to drugs. Third, this method could be further exploited to compare the intrinsic activity of antibiotics *in vivo* in embryos infected with the three species of the *M. abscessus* complex, *M. abscessus sensu stricto*, *Mycobacterium massiliense*, and *Mycobacterium bolletii*, which are known to respond differently to antibiotics *in vitro* (41, 42).

Finally, the ZF embryo is particularly suited for high-throughput screening, as shown recently for *Mycobacterium marinum* (36, 43, 44). Work is currently in progress in our laboratory to develop an *in vivo* platform for high-throughput screening of molecules against *M. abscessus* in order to speed up the process of identifying promising drug candidates, particularly warranted due to the extreme resistance of *M. abscessus* to most current antibiotics.

REFERENCES

1. **Medjahed H, Gaillard JL, Reyrat JM.** 2010. *Mycobacterium abscessus*: a new player in the mycobacterial field. Trends Microbiol. **18**:117–123. http://dx.doi.org/10.1016/j.tim.2009.12.007.
2. **Petrini B.** 2006. *Mycobacterium abscessus*: an emerging rapid-growing potential pathogen. Apmis **114**:319–328. http://dx.doi.org/10.1111/j.1600-0463.2006.apm_390.x.
3. **Roux AL, Catherinot E, Ripoll F, Soismier N, Macheras E, Ravilly S, Bellis G, Vibet MA, Le Roux E, Lemonnier L, Gutierrez C, Vincent V, Fauroux B, Rottman M, Guillemot D, Gaillard JL.** 2009. Multicenter study of prevalence of nontuberculous mycobacteria in patients with cystic fibrosis in France. J. Clin. Microbiol. **47**:4124–4128. http://dx.doi.org/10.1128/JCM.01257-09.
4. **Sanguinetti M, Ardito F, Fiscarelli E, La Sorda M, D'Argenio P, Ricciotti G, Fadda G.** 2001. Fatal pulmonary infection due to multidrug-resistant *Mycobacterium abscessus* in a patient with cystic fibrosis. J. Clin. Microbiol. **39**:816–819. http://dx.doi.org/10.1128/JCM.39.2.816-819.2001.
5. **Gilljam M, Schersten H, Silverborn M, Jonsson B, Ericsson Hollsing A.** 2010. Lung transplantation in patients with cystic fibrosis and *Mycobacterium abscessus* infection. J. Cyst. Fibros. **9**:272–276. http://dx.doi.org/10.1016/j.jcf.2010.03.008.
6. **Aitken ML, Limaye A, Pottinger P, Whimbey E, Goss CH, Tonelli MR, Cangelosi GA, Dirac MA, Olivier KN, Brown-Elliott BA, McNulty S, Wallace RJ, Jr.** 2012. Respiratory outbreak of *Mycobacterium abscessus* subspecies *massiliense* in a lung transplant and cystic fibrosis center. Am. J.

Respir. Crit. Care Med. **185:**231–232. http://dx.doi.org/10.1164/ajrccm .185.2.231.

7. **Wallace RJ, Jr, Brown BA, Griffith DE.** 1998. Nosocomial outbreaks/ pseudo-outbreaks caused by nontuberculous mycobacteria. Annu. Rev. Microbiol. **52:**453–490. http://dx.doi.org/10.1146/annurev.micro.52.1 .453.

8. **Viana-Niero C, Lima KV, Lopes ML, Rabello MC, Marsola LR, Brilhante VC, Durham AM, Leao SC.** 2008. Molecular characterization of *Mycobacterium massiliense* and *Mycobacterium bolletii* in isolates collected from outbreaks of infections after laparoscopic surgeries and cosmetic procedures. J. Clin. Microbiol. **46:**850–855. http://dx.doi.org/10.1128 /JCM.02052-07.

9. **Zelazny AM, Root JM, Shea YR, Colombo RE, Shamputa IC, Stock F, Conlan S, McNulty S, Brown-Elliott BA, Wallace RJ, Jr, Olivier KN, Holland SM, Sampaio EP.** 2009. Cohort study of molecular identification and typing of *Mycobacterium abscessus*, *Mycobacterium massiliense*, and *Mycobacterium bolletii*. J. Clin. Microbiol. **47:**1985–1995. http://dx.doi .org/10.1128/JCM.01688-08.

10. **Cullen AR, Cannon CL, Mark EJ, Colin AA.** 2000. *Mycobacterium abscessus* infection in cystic fibrosis. Colonization or infection? Am. J. Respir. Crit. Care Med. **161:**641–645. http://dx.doi.org/10.1164/ajrccm .161.2.9903062.

11. **Tomashefski JF, Jr, Stern RC, Demko CA, Doershuk CF.** 1996. Nontuberculous mycobacteria in cystic fibrosis. An autopsy study. Am. J. Respir. Crit. Care Med. **154:**523–528. http://dx.doi.org/10.1164 /ajrccm.154.2.8756832.

12. **Rodriguez G, Ortegon M, Camargo D, Orozco LC.** 1997. Iatrogenic *Mycobacterium abscessus* infection: histopathology of 71 patients. Br. J. Dermatol. **137:**214–218. http://dx.doi.org/10.1046/j.1365-2133.1997 .18081891.x.

13. **Griffith DE, Aksamit T, Brown-Elliott BA, Catanzaro A, Daley C, Gordin F, Holland SM, Horsburgh R, Huitt G, Iademarco MF, Iseman M, Olivier K, Ruoss S, von Reyn CF, Wallace RJ, Jr, Winthrop K.** 2007. An official ATS/IDSA statement: diagnosis, treatment, and prevention of nontuberculous mycobacterial diseases. Am. J. Respir. Crit. Care Med. **175:**367–416. http://dx.doi.org/10.1164/rccm.200604-571ST.

14. **Jeon K, Kwon OJ, Lee NY, Kim BJ, Kook YH, Lee SH, Park YK, Kim CK, Koh WJ.** 2009. Antibiotic treatment of *Mycobacterium abscessus* lung disease: a retrospective analysis of 65 patients. Am. J. Respir. Crit. Care Med. **180:**896–902. http://dx.doi.org/10.1164/rccm.200905-0704OC.

15. **De Groote MA, Johnson L, Podell B, Brooks E, Basaraba R, Gonzalez-Juarrero M.** 2013. GM-CSF knockout mice for preclinical testing of agents with antimicrobial activity against *Mycobacterium abscessus*. J. Antimicrob. Chemother. **69:**1057–1064. http://dx.doi.org/10.1093/jac /dkt451.

16. **Lerat I, Cambau E, Roth Dit Bettoni R, Gaillard JL, Jarlier V, Truffot C, Veziris N.** 2013. *In vivo* evaluation of antibiotic activity against *Mycobacterium abscessus*. J. Infect. Dis. **209:**905–912. http://dx.doi.org/10.1093 /infdis/jit614.

17. **Lavollay M, Dubee V, Heym B, Herrmann JL, Gaillard JL, Gutmann L, Arthur M, Mainardi JL.** 11 November 2013. *In vitro* activity of cefoxitin and imipenem against *Mycobacterium abscessus* complex. Clin. Microbiol. Infect. http://dx.doi.org/10.1111/1469-0691.12405.

18. **Cortes M, Singh AK, Reyrat JM, Gaillard JL, Nassif X, Herrmann JL.** 2011. Conditional gene expression in *Mycobacterium abscessus*. PLoS One **6:**e29306. http://dx.doi.org/10.1371/journal.pone.0029306.

19. **Bernut A, Herrmann JL, Kissa K, Dubremetz JF, Gaillard JL, Lutfalla G, Kremer L.** 2014. *Mycobacterium abscessus* cording prevents phagocytosis and promotes abscess formation. Proc. Natl. Acad. Sci. U. S. A. **111:**E943– E952. http://dx.doi.org/10.1073/pnas.1321390111.

20. **Talati NJ, Rouphael N, Kuppalli K, Franco-Paredes C.** 2008. Spectrum of CNS disease caused by rapidly growing mycobacteria. Lancet Infect. Dis. **8:**390–398. http://dx.doi.org/10.1016/S1473-3099(08)70127-0.

21. **Lee MR, Cheng A, Lee YC, Yang CY, Lai CC, Huang YT, Ho CC, Wang HC, Yu CJ, Hsueh PR.** 2011. CNS infections caused by *Mycobacterium abscessus* complex: clinical features and antimicrobial susceptibilities of isolates. J. Antimicrob. Chemother. **67:**222–225. http://dx.doi.org/10 .1093/jac/dkr420.

22. **Rottman M, Catherinot E, Hochedez P, Emile JF, Casanova JL, Gaillard JL, Soudais C.** 2007. Importance of T cells, gamma interferon, and tumor necrosis factor in immune control of the rapid grower *Mycobacterium abscessus* in C57BL/6 mice. Infect. Immun. **75:**5898–5907. http://dx.doi .org/10.1128/IAI.00014-07.

23. **Catherinot E, Clarissou J, Etienne G, Ripoll F, Emile JF, Daffe M, Perronne C, Soudais C, Gaillard JL, Rottman M.** 2007. Hypervirulence of a rough variant of the *Mycobacterium abscessus* type strain. Infect. Immun. **75:**1055–1058. http://dx.doi.org/10.1128/IAI.00835-06.

24. **Woods GL, Brown-Elliott BA, Conville PS, Desmond EP, Hall GS, Lin G, Pfyffer GE, Ridderhof JC, Siddiqi SH, Wallace RJ, Warren NG, Witebsky FG.** 2011. Susceptibility testing of mycobacteria, nocardiae, and other aerobic actinomycetes; approved standard—second edition. M24-A2. CLSI, Wayne, PA.

25. **Lamason RL, Mohideen MA, Mest JR, Wong AC, Norton HL, Aros MC, Jurynec MJ, Mao X, Humphreville VR, Humbert JE, Sinha S, Moore JL, Jagadeeswaran P, Zhao W, Ning G, Makalowska I, McKeigue PM, O'Donnell D, Kittles R, Parra EJ, Mangini NJ, Grunwald DJ, Shriver MD, Canfield VA, Cheng KC.** 2005. SLC24A5, a putative cation exchanger, affects pigmentation in zebrafish and humans. Science **310:**1782– 1786. http://dx.doi.org/10.1126/science.1116238.

26. **Adams KN, Takaki K, Connolly LE, Wiedenhoft Winglee K, Humbert O, Edelstein PH, Cosma CL, Ramakrishnan L.** 2011. Drug tolerance in replicating mycobacteria mediated by a macrophage-induced efflux mechanism. Cell **145:**39–53. http://dx.doi.org/10.1016/j.cell.2011.02.022.

27. **Lavollay M, Fourgeaud M, Herrmann JL, Dubost L, Marie A, Gutmann L, Arthur M, Mainardi JL.** 2011. The peptidoglycan of *Mycobacterium abscessus* is predominantly cross-linked by L,D-transpeptidases. J. Bacteriol. **193:**778–782. http://dx.doi.org/10.1128/JB.00606-10.

28. **Medjahed H, Reyrat JM.** 2009. Construction of *Mycobacterium abscessus* defined glycopeptidolipid mutants: comparison of genetic tools. Appl. Environ. Microbiol. **75:**1331–1338. http://dx.doi.org/10.1128/AEM .01914-08.

29. **Howard ST, Rhoades E, Recht J, Pang X, Alsup A, Kolter R, Lyons CR, Byrd TF.** 2006. Spontaneous reversion of *Mycobacterium abscessus* from a smooth to a rough morphotype is associated with reduced expression of glycopeptidolipid and reacquisition of an invasive phenotype. Microbiology **152:**1581–1590. http://dx.doi.org/10.1099/mic.0.28625-0.

30. **Zelmer A, Carroll P, Andreu N, Hagens K, Mahlo J, Redinger N, Robertson BD, Wiles S, Ward TH, Parish T, Ripoll J, Bancroft GJ, Schaible UE.** 2012. A new *in vivo* model to test anti-tuberculosis drugs using fluorescence imaging. J. Antimicrob. Chemother. **67:**1948–1960. http://dx.doi.org/10.1093/jac/dks161.

31. **Andreu N, Zelmer A, Sampson SL, Ikeh M, Bancroft GJ, Schaible UE, Wiles S, Robertson BD.** 2013. Rapid *in vivo* assessment of drug efficacy against *Mycobacterium tuberculosis* using an improved firefly luciferase. J. Antimicrob. Chemother. **68:**2118–2127. http://dx.doi.org/10.1093/jac /dkt155.

32. **Byrd TF, Lyons CR.** 1999. Preliminary characterization of a *Mycobacterium abscessus* mutant in human and murine models of infection. Infect. Immun. **67:**4700–4707.

33. **Oh CT, Moon C, Jeong MS, Kwon SH, Jang J.** 2013. *Drosophila melanogaster* model for *Mycobacterium abscessus* infection. Microbes Infect. **15:**788–795. http://dx.doi.org/10.1016/j.micinf.2013.06.011.

34. **Oh CT, Moon C, Park OK, Kwon SH, Jang J.** 2014. Novel drug combination for *Mycobacterium abscessus* disease therapy identified in a *Drosophila* infection model. J. Antimicrob. Chemother. **69:**1599–1607. http: //dx.doi.org/10.1093/jac/dku024.

35. **Squiban B, Kurz CL.** 2011. *C. elegans*: an all in one model for antimicrobial drug discovery. Curr. Drug Targets **12:**967–977. http://dx.doi.org/10 .2174/138945011795677854.

36. **Takaki K, Cosma CL, Troll MA, Ramakrishnan L.** 2012. An *in vivo* platform for rapid high-throughput antitubercular drug discovery. Cell Rep. **2:**175–184. http://dx.doi.org/10.1016/j.celrep.2012.06.008.

37. **Takaki K, Davis JM, Winglee K, Ramakrishnan L.** 2013. Evaluation of the pathogenesis and treatment of *Mycobacterium marinum* infection in zebrafish. Nat. Protoc. **8:**1114–1124. http://dx.doi.org/10.1038/nprot .2013.068.

38. **Miyasaka T, Kunishima H, Komatsu M, Tamai K, Mitsutake K, Kanemitsu K, Ohisa Y, Yanagisawa H, Kaku M.** 2007. *In vitro* efficacy of imipenem in combination with six antimicrobial agents against *Mycobacterium abscessus*. Int. J. Antimicrob. Agents **30:**255–258. http://dx.doi.org /10.1016/j.ijantimicag.2007.05.003.

39. **Shen GH, Wu BD, Hu ST, Lin CF, Wu KM, Chen JH.** 2010. High efficacy of clofazimine and its synergistic effect with amikacin against rapidly growing mycobacteria. Int. J. Antimicrob. Agents **35:**400–404. http: //dx.doi.org/10.1016/j.ijantimicag.2009.12.008.

40. **Phennicie RT, Sullivan MJ, Singer JT, Yoder JA, Kim CH.** 2010. Specific

resistance to *Pseudomonas aeruginosa* infection in zebrafish is mediated by the cystic fibrosis transmembrane conductance regulator. Infect. Immun. **78:**4542–4550. http://dx.doi.org/10.1128/IAI.00302-10.

41. **Bastian S, Veziris N, Roux AL, Brossier F, Gaillard JL, Jarlier V, Cambau E.** 2011. Assessment of clarithromycin susceptibility in strains belonging to the *Mycobacterium abscessus* group by *erm*(*41*) and *rrl* sequencing. Antimicrob. Agents Chemother. **55:**775–781. http://dx.doi.org/10.1128/AAC.00861-10.

42. **Kim HY, Kim BJ, Kook Y, Yun YJ, Shin JH, Kim BJ, Kook YH.** 2010. *Mycobacterium massiliense* is differentiated from *Mycobacterium abscessus* and *Mycobacterium bolletii* by erythromycin ribosome methyltransferase

gene (*erm*) and clarithromycin susceptibility patterns. Microbiol. Immunol. **54:**347–353. http://dx.doi.org/10.1111/j.1348-0421.2010.00221.x.

43. **Carvalho R, de Sonneville J, Stockhammer OW, Savage ND, Veneman WJ, Ottenhoff TH, Dirks RP, Meijer AH, Spaink HP.** 2011. A high-throughput screen for tuberculosis progression. PLoS One **6:**e16779. http://dx.doi.org/10.1371/journal.pone.0016779.

44. **Spaink HP, Cui C, Wiweger MI, Jansen HJ, Veneman WJ, Marin-Juez R, de Sonneville J, Ordas A, Torraca V, van der Ent W, Leenders WP, Meijer AH, Snaar-Jagalska BE, Dirks RP.** 2013. Robotic injection of zebrafish embryos for high-throughput screening in disease models. Methods **62:**246–254. http://dx.doi.org/10.1016/j.ymeth.2013.06.002.